Bulletin of the Seismological Society of America, Vol. 89, No. 1, pp. 202–214, February 1999

Using a Genetic Algorithm to Model Broadband Regional Waveforms for Crustal Structure in the Western United States

by Joydeep Bhattacharyya,* Anne F. Sheehan, Kristy Tiampo, and John Rundle

Abstract In this study, we analyze regional seismograms to obtain the crustal structure in the eastern Great Basin and western Colorado plateau. Adopting a forward-modeling approach, we develop a genetic algorithm (GA) based parameter search technique to constrain the one-dimensional crustal structure in these regions. The data are broadband three-component seismograms recorded at the 1994–95 IRIS PASSCAL Colorado Plateau to Great Basin experiment (CPGB) stations and supplemented by data from U.S. National Seismic Network (USNSN) stations in Utah and Nevada. We use the southwestern Wyoming mine collapse event (M_b = 5.2) that occurred on 3 February 1995 as the seismic source. We model the regional seismograms using a four-layer crustal model with constant layer parameters. Timing of teleseismic receiver functions at CPGB stations are added as an additional constraint in the modeling.

GA allows us to efficiently search the model space. A carefully chosen fitness function and a windowing scheme are added to the algorithm to prevent search stagnation. The technique is tested with synthetic data, both with and without random Gaussian noise added to it. Several separate model searches are carried out to estimate the variability of the model parameters. The average Colorado plateau crustal structure is characterized by a 40-km-thick crust with velocity increases at depths of about 10 and 25 km and a fast lower crust while the Great Basin has approximately 35-km-thick crust and a 2.9-km-thick sedimentary layer.

Introduction

Crustal structure of the Colorado plateau and the Basin and Range provinces of the western United States has been a subject of considerable debate for the last three decades. Several seismological data types, including receiver functions, refraction profiles, body and surface waveforms, and travel times, have been used to constrain the average one-dimensional velocity structure in these regions (Roller, 1965; Keller *et al.*, 1979; Priestley and Brune, 1978; Wolf and Cipar, 1993; Ozalaybey *et al.*, 1997; Song *et al.*, 1996; Sheehan *et al.*, 1997). These studies have presented varying estimates of crustal thickness and the depth to the crustal discontinuities. The difference between these estimates can be attributed to the different spatial sampling of the studies coupled with various assumptions adopted in each of the analyses. Recent availability of high dynamic-range, digital broadband instrumentation enables us to greatly improve our ability to estimate seismic parameters from regional seismograms. These seismograms have been shown to be strongly sensitive to the crust and lithospheric structure (e.g., Song *et al.*, 1996; Rodgers and Schwartz, 1997, 1998; Ozalaybey *et al.*, 1997). Use of improved analytical and computational tools, for example, computing source parameters and synthetic seismograms, let us remove some of the assumptions made during the analysis and improve signal extraction. Moreover, availability of portable high-quality three-component seismometers allow us to rapidly increase the spatial sampling of our data, thereby letting us investigate unexplored regions.

In principle, modeling that makes use of the whole seismic waveform, including both body waves and surface-wave modes, should have advantages over methods that use only narrowly selected parts of seismograms, such as arrival times or phase velocities. Full waveform modeling also allows us to use information contained in higher modes without having to explicitly identify those modes. This modeling technique does not require the station density required by body-wave tomography and has increased sensitivity to crustal structure over teleseismic phase velocities. Thus, it is a technique ideally suited for regional deployments of broadband sensors such as the Colorado plateau to Great Basin PASSCAL ex-

*Present address: Department of Geology and Geophysics, Yale University, New Haven, Connecticut 06511. E-mail: joydeep@hess.geology.yale.edu.

periment (Jones *et al.*, 1996). By including both radial and vertical waveforms in our modeling, we obtain increased sensitivity to *SV* and reduce the chances of modeling noise coherent on only one channel. Finally, our complete waveform modeling technique allows for phase conversions due to the intracrustal layers and for regional waveforms increases the delineation of thin crustal layers.

In this study, we adopt a forward-modeling approach to constrain the crustal structure in both the Colorado plateau and the Great Basin provinces. A simple crustal model is adopted, and synthetic seismograms are computed for these models. We search the solution space using a large number of models and select the model that best fits the synthetics to the recorded data using some fitness measure. We adopt the reflectivity technique (Randall, 1994) to compute the synthetics. For the search algorithm, we adopt the genetic algorithm (GA) modeling technique in this study. Many seismological optimization problems are nonlinear and result in irregular fitness functions. Moreover, they can have a rough fitness landscape with several local minima. Thus, local optimization techniques, such as linearized matrix inversion, steepest descent, and conjugate gradients, can converge prematurely to a local minima. In addition, the success in obtaining an optimum solution can depend strongly on the choice of the starting model. To mitigate these problems, global optimization techniques that avoid these limitations are particularly useful in seismology. GA is such a technique that allows us to efficiently search the model space and converge toward a global minima. Using these tools, we have developed a parameter estimation technique that lets us rapidly model the one-dimensional crustal structure using three-component broadband seismograms.

In the following sections, we first discuss the data and the sensitivity of the various model parameters on the data. Next, we develop the GA search scheme and test our technique with synthetic data with various levels of noise added in. This step allows us to estimate the robustness of our technique. Finally, this method is used to model the crustal structure in the Colorado plateau and Great Basin provinces.

Dataset

The seismograms used in this study come from the Colorado plateau–Great Basin (CPGB) deployment of 11 broadband portable sensors in Colorado and Utah from October 1994 to July 1995 (Jones *et al.*, 1996; Sheehan *et al.*, 1997). Broadband recordings from nearby U.S. National Seismic Network (USNSN) stations Battle Mountain, Nevada (BMN), Kanab, Utah (KNB), Elko, Nevada (ELK), and Mina, Nevada (MNV), have been added to this dataset. The station locations are shown in Figure 1. In this study, waveforms from the mine collapse event in southwestern Wyoming (Pechmann *et al.*, 1995) are modeled. The seismic event (M_b = 5.2) occurred on 3 February 1995, 29 km west of the town of Green River, Wyoming (Fig. 1). This is a well-modeled event and is within 140 to 800 km of the CPGB stations. The use of a well-calibrated source minimizes the biasing effects of unmodeled source signature in the estimation of seismic structure. Pechmann *et al.* (1995) have concluded that the seismic source can be represented as a 0.5-km-deep mine collapse event. Therefore, with a shallow source depth and for regional propagation distances, the body waves and the surface waves recorded in the early part of the seismogram (and used in this study) primarily travel through the crust and can constrain the average crustal structure. The accurate determination of both the source location and origin time allows us to estimate correctly the arrival times of the body and surface waves.

Both the CPGB and the USNSN stations recorded the event on three components. No clear arrival is observed in the transverse component, primarily due to the implosional nature of the source. This point has also been noted by Pechmann *et al.* (1995). Therefore, in this study, we model the vertical and the radial components that can be adequately combined to investigate high-resolution one-dimensional crustal structure (Song *et al.*, 1996). We add that, in earthquake events, the technique described in this article can readily incorporate the transverse-component data and thereby improve the shear velocity model.

The recorded seismograms are first instrument deconvolved and integrated to displacement. This is important because it allows us to combine recordings made using different instrument types and also allows us to extend the data to longer periods. For example, clear signals are observed up to 40 sec while the long-period roll offs for the CPGB instruments are typically at 30 sec. Next, a third-order zero-phase Butterworth filter is applied with a bandpass between 10 and 50 sec. The particular frequency cutoffs are used primarily for two reasons: (a) the high-frequency features in the seismogram are not modeled in this study because they can strongly be affected by lateral variations of elastic properties and thereby bias the one-dimensional model; (b) signals at very long periods had to be removed because noise levels are amplified at these periods due to instrument deconvolution, thereby severely contaminating the signal. The radial- and vertical-component seismograms used in this study are shown in Figure 2. We can observe clearly the Rayleigh waves in the seismograms, and as expected for the collapse-source mechanism, Love waves are absent for this event. We have concentrated our modeling efforts on the Rayleigh waves because of two reasons: (a) these waves are the most prominent arrival observed in the data (Fig. 2) and are thus expected to have a large signal-to-noise ratio; (b) these waveforms have simple wave shapes and can be fit using simple 1D crustal models. However, the waveform fitting technique used in this study is capable of modeling the complete waveform, that is, body waves and surface waves. The data window is selected by marking the moveout velocities, isolates the Rayleigh wave (Fig. 2). These moveout velocities are also used to excise the Rayleigh waveform from the synthetics, thereby preserving the duration

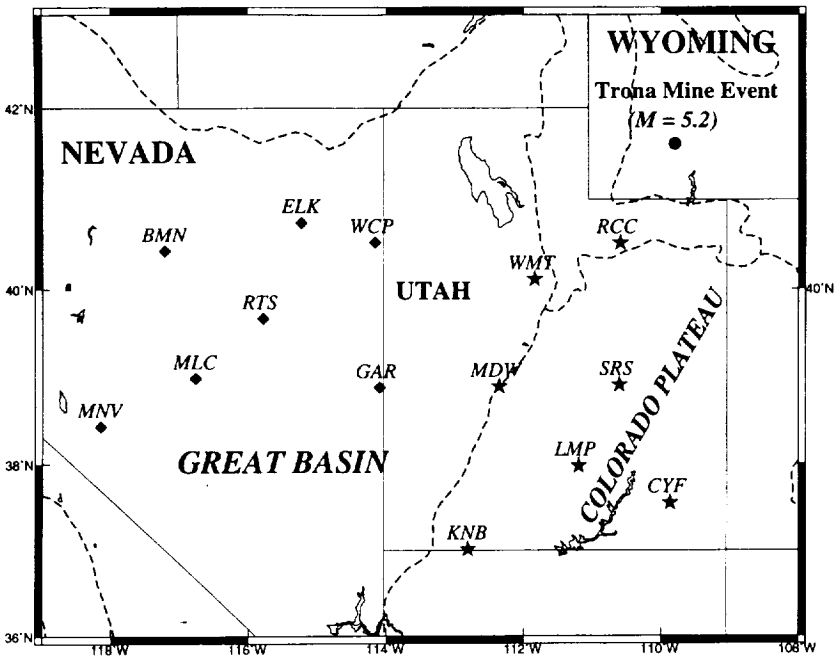

Figure 1. Location of the 3 February 1995 mine-collapse event and the seismic stations at regional distances used in this study. Stations BMN, DUG, ELK, KNB, and MNV belong to the U.S. National Seismic Network (USNSN), and the rest of the stations are from the Colorado plateau to Great Basin (CPGB) PASSCAL experiment. The diamonds indicate stations used for estimating Great Basin crustal structure, and stars indicate stations used for modeling the Colorado plateau crust. Solid lines denote state boundaries, and dashed lines show boundaries between geologic provinces.

and the arrival-time information when the synthetics are compared to the data. We use a conservative window size that allows for variable arrival times due to laterally varying seismic structure and dispersion. Typically, the extracted waveforms are 35 to 50 sec long. The vertical lines in Figure 2 show the seismograms and the data window used in this study.

Model Sensitivities

Given an accurate source location and mechanism, a usual problem for waveform modeling is to understand the sensitivity of the data to the model parameters. Moreover, regional seismograms produced by shallow events, like the one used in this study, can be very complicated (e.g., Song *et al.*, 1996). To better understand these effects, we have carried out simple tests using synthetic seismograms computed using different one-dimensional crustal models. Our goal is to identify the parameters in the model that the data are sensitive to and allow variations only in those parameters in the modeling procedure. To simulate real data analyzed in this study, we carried out these tests using reflectivity synthetics (Randall, 1994), and we used the moment tensor source presented for this event by Pechmann *et al.*, 1995. We have used a one-dimensional velocity model given by Wolf and Cipar (1993) that is derived from refraction lines across southeastern Utah and northeastern Arizona. The model, inverted from the Chinle-to-Hanksville line, essentially consists of three crustal layers of constant layer velocity and thicknesses. We have slightly modified this model by adding a sedimentary layer. Simplified models are developed by varying each of the model parameters separately, isolating the sensitivity of the synthetics to each of them. The radial- and vertical-component synthetics are filtered to periods between 10 and 50 sec to make them consistent with the recorded seismograms. Following Patton and Taylor (1984), the shear-wave attenuation (Q_β) in the crust is fixed to 100, and we use a scaling ratio of Q_α:Q_β equal to 2. Finally, the synthetics are computed for distance ranges of 200 to 900 km, encompassing the source-to-receiver distances used in our study.

We have carried out a number of experiments to estimate separately the effect of layer velocities, thicknesses, Poisson's ratio, and densities. By systematically varying the velocities of the sediment layer, upper and lower crust, and upper mantle, we tested the sensitivity of the synthetic seismograms to these parameters. From these experiments, we find that these shallow source waveforms are strongly affected by the sediment layer and the upper crustal layer velocities, are affected by the lower crust at larger distances (probably due to their increased depth of penetration), and are insensitive to the uppermost mantle velocity. Because we use a fixed *Vp*:*Vs* ratio, changing *P*-wave velocities effectively modifies the *S*-wave velocities too. Changing layer thicknesses had a similar effect and therefore can trade off with the velocities in the fitting process. The synthetics are slightly affected by the density of the crust and insensitive to upper mantle density variations. We vary Poisson's ratio between 1.73 and 1.82, thereby covering the range of possible continental values (Rudnick and Fountain, 1995; Christensen and Mooney, 1995; Christensen, 1996); this factor slightly affects the synthetics. The synthetics are sensitive to the total crustal thickness at distances larger than 300 km. We conclude from these tests that the synthetics are mostly sensitive to the shallow layers (approximately 0 to 30 km), a point also noted in Song *et al.* (1996). We also note that

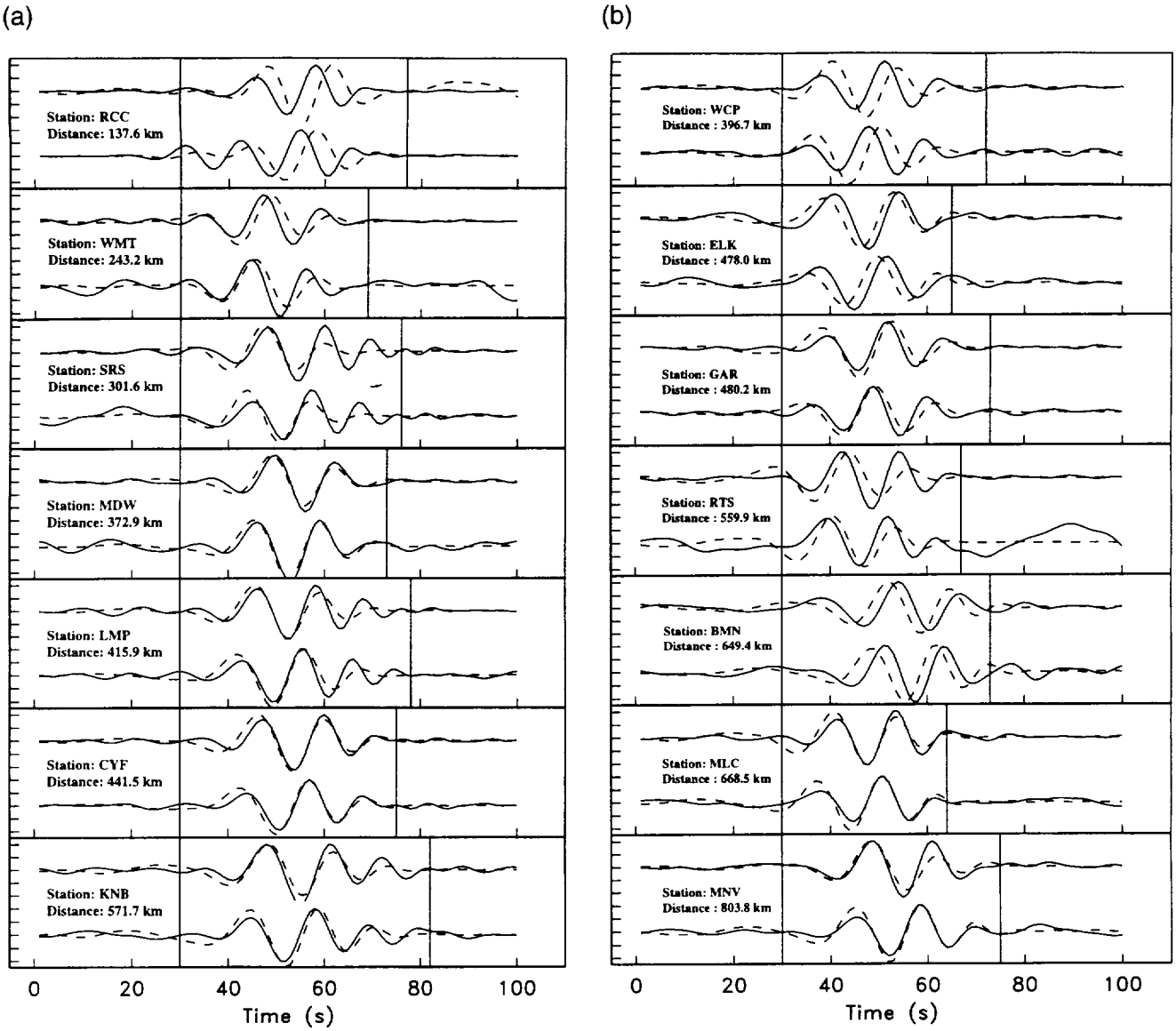

Figure 2. (a) The vertical- and radial-component seismograms used in this study to estimate Colorado plateau crustal structure. The solid lines show the recorded seismograms that have been instrument deconvolved to displacement and bandpass filtered between periods 10, and 50 sec. For each station, the upper traces are from vertical-component seismograms, and the lower trace is radial component. The vertical lines indicate the portion of the seismograms used for waveform fitting, and the source-to-receiver distance is shown for each station. Each of the seismograms are normalized to their maximum amplitudes. The dashed lines show the synthetic waveforms predicted by our best-fitting one-dimensional crustal model for this region. Note that the recorded seismograms are slightly slower than those predicted by our model for stations CYF, LMP, and SRS and faster for stations WMT and RCC. (b) Similar to Figure 2a, but for stations used in modeling the crustal structure of the Great Basin province. We note that the seismograms recorded at stations BMN and ELK are slightly slower and seismograms at WCP and RTS are slightly faster than those predicted by our average model.

the seismograms are not sensitive to the uppermost mantle structure. Because we do not have a complete data coverage, trade-offs between model parameters can occur. To diminish these effects, we allow variation in model parameters within prescribed limits whose values are based on published results from the study regions. Also, these trade-offs can give rise to several local minima; GA is capable of identifying the global minimum in such a situation (Goldberg, 1989). Based on these tests, it can be concluded that the data are adequate to model for four crustal layers, which includes a thin sedimentary layer. However, it is stressed that the whole crust in the western United States is not as simple as our 1D models (Hearn *et al.*, 1991; Wolf and Cipar, 1993; Sheehan *et al.*, 1997). Our goal in this study is to develop a technique

that can rapidly obtain an average 1D regional model and is consistent with the relatively long-period data (10 to 50 sec).

Use of Genetic Algorithms in Seismic Waveform Modeling

In recent years, GA have been employed in the solution of nonlinear optimization problems in the physical sciences. Most geophysical modeling problems are traditionally solved using local optimization techniques, such as linearized matrix inversion, steepest descent, conjugate gradients, or grid search techniques. These techniques can sometimes converge prematurely to a local minima, and success can depend strongly on the choice of a starting model. A global optimization technique such as a GA mitigates these problems and are an attractive search tool suitable for the irregular, multimodal fitness functions typically observed in modeling seismic waveforms. Since a GA undergoes an initially random and progressively more deterministic sampling of the parameter space, these algorithms offer the possibility of efficiently and relatively rapidly locating the most promising regions of the solution space. Their ability to solve nonlinear, nonlocal optimization problems without *a priori* knowledge of curvature information precludes the need for derivative computations, a particularly important feature because it allows for fast approximate forward modeling where no exact derivative information is available (Wright, 1991). Because genetic algorithms sample the space directly, linearization of the problem is unnecessary, thus avoiding errors involved in this approximation. Use of synthetic seismograms for modeling seismic waveforms, which involves the nonlinear interaction of model parameters, is an obvious application of this feature.

Several recent studies have employed GAs to invert for seismic structure (Stoffa and Sen, 1991; Sen and Stoffa, 1992; Stoffa *et al.*, 1994; Boschetti *et al.*, 1996), hypocenter relocation (Billings *et al.*, 1994), seismic phase alignment (Winchester *et al.*, 1993), fault-zone geometry (Yu, 1995), mantle velocity structure (Neves *et al.*, 1996; Curtis *et al.*, 1995; Lomax and Snieder, 1995), and crustal velocity structure (Jin and Madariaga, 1993; Drijkoningen and White, 1995; Zhou *et al.*, 1995). Our modeling of seismic structure in the Colorado plateau and eastern Great Basin will use a GA as shown in Figure 3. The program employs a random number generator to produce an initial set of 100 potential values for each of the waveform parameters, within an initially specified range of acceptable values. These model values are then coded as genes, which in turn are combined to form specific models, or chromosomes, for each member of the initial population of 100 potential solutions. These models are ranked, from the best to the worst, according to a fitness function, which is obtained from the cross-correlation function computed between each synthetic and the recorded seismograms. We do not shift the waveforms in time to improve the fit. This procedure preserves the absolute travel time of the Rayleigh waves and, because the mine collapse origin time is well constrained (Pechmann *et al.*, 1995), provides an important constraint on the velocity structure. The models with the highest cumulative correlation coefficient (used in this study as a fitness measure and described later) are the fittest and are selected, based on their relative fitness, to contribute to the next generation, where the genetic operations of crossover and mutation take place (Wright, 1991; Michalewicz, 1996). Between each subsequent generation of the GA, a crossover operation occurs, in which two randomly selected members of the new population swap genes based on a randomly generated position in the string. The parent models are recombined, with the left portion of one parent and the right portion of the other parent creating one new model, or offspring, of the correct length. The corresponding recombination on the remaining subchromosomes creates a second offspring. In two-point crossover, the parents are split at two randomly selected locations in the parent models, with everything to the right of the first location in one parent recombining with everything to the left of the same location in the second parent, while the second offspring is generated from everything to the left of the second location in the first parent and everything to the right of that same location in

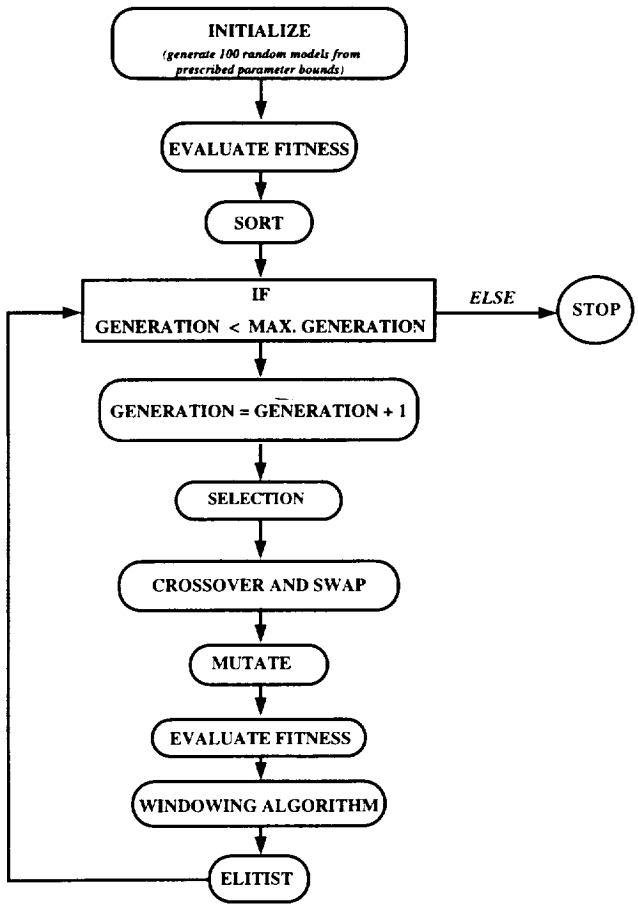

Figure 3. The flowchart of the genetic algorithm adopted in this study. The individual steps are discussed in the text.

the second parent (Michalewicz). Crossover is the device by which the random information exchange takes place—new members with different fitness are generated in order to evolve our directed search. In a GA, mutation corresponds to the replacement of a gene, that is, a model parameter, by a new, randomly generated value. Mutation is done to explore random parts of the model space that might have been otherwise missed.

Each model parameter is represented by an array of real values (Wright, 1991). The CPU intensive nature of the particular fitness function employed for the waveform modeling and the necessity for high precision calculations makes the use of a real-valued GA very attractive. We use an elitist function in this algorithm that ensures that the best member of all populations, current and prior, is stored in memory and then copied into each current population, where it might otherwise no longer exist (Michalewicz, 1996). To avoid search stagnation, a windowing function was added to the GA. Significant trade-offs between the crustal seismic properties can result in a rough fitness landscape with numerous local minima. This particular fitness landscape can generate a population with a small standard deviation of the population fitness after only a relatively few generations. This can decrease the selection pressure toward better structures, causing the search to stagnate and even reach premature convergence in several instances. As a result, we created a routine to window the fitness by subtracting the fitness value of the worst member of the previous generation from every new population fitness, prior to selecting the next generation. This ensured that those members with a better relative fitness were included in a greater proportion in the next generation, despite the small absolute difference in their fitness.

Features of the Waveform Modeling

Modeling Constraints. As described earlier, several recent studies have modeled the crustal structure of the Colorado plateau and the Great Basin provinces. Constraints on the seismic structure from these studies can greatly improve the search algorithm. The constraints help us primarily by (a) reducing trade-offs between model parameters, (b) decreasing the possibility of converging to a local minima, and (c) increasing the convergence rate by allowing us to consider a subset of the models. The following constraints have been used in the GA modeling.

1. Receiver function constraints on the *Ps* times. The *Ps* times are defined as the travel time difference between the direct *P* and the converted *S* wave resulting from the interaction of the *P* wave with the Moho under a given station. The *Ps* times used here are obtained from the study of Sheehan *et al.* (1997). The *Ps* time for a crustal model can be calculated from the average *P* and *S* velocities, crustal thickness, and an average ray parameter for the incoming *P* wave (Zandt *et al.*, 1995). The observed *Ps* times for stations in the Great Basin and Colorado plateau provinces are 4.2 ± 0.4 sec and 5.1 ± 0.4 sec, respectively (Sheehan *et al.*, 1997). In this study, we limit our search to models that produce theoretical *Ps* times within these limits. In conjunction with average crustal velocity, this constraint can improve our estimate of the total crustal thickness.
2. V_p:V_s ratio. In the GA modeling, we use a fixed V_p:V_s ratio. For the sedimentary layer, this value equals 1.73 (Poisson's ratio = 0.25), and for the rest of the crust, we use 1.77 (Poisson's ratio = 0.265), following the results of Schneider (1997).
3. Density. The densities for the crustal layers are calculated using the empirical relation $\rho = 0.252 + 0.3788 \times V_p$ (Nafe and Drake, 1957). This constraint has also been successfully used in several recent western U.S. crustal studies (Wolf and Ciper, 1993).
4. Upper mantle velocity. In a recent study, Schneider (1997) analyzed the surface-wave phase velocity curves to explicitly model for the upper mantle shear-wave velocity in this region. These phase velocity data provide better constraints on the uppermost mantle velocity than our data, and we use the *Pn* velocity estimate from this study in our modeling. Briefly, we have fixed the uppermost mantle *P*-wave velocity in our model to 7.9 km/sec and use an uppermost mantle *S*-wave velocity of 4.46 km/sec.

Input Parameters. The following parameters are set *a priori* in the modeling algorithm and have the same value in each generation:

1. Probability of crossover. We tested the convergence for both one- and two-point crossover schemes and found their rates to be similar, producing nearly the same model solutions. We thus use both of these variations of GA in our modeling. The crossover probability was set based on tests run on synthetic data to determine the best convergence for different crossover rates.
2. Probability of mutation. This probability value controls the number of times mutation occurs in a given population, that is, for models in a particular generation. This value can be optimally set to equal $1/n$, the number of model parameters (Bäck, 1996). In this study, n is equal to 8.
3. Range of model parameters. The algorithm chosen for this study randomly searches for model parameters within a prescribed range of values. Unrealistic model parameters can lead to inordinately large model spaces, thus leading to slower convergence.

The Fitness Function Value. In this algorithm, we seek the model that produces synthetics that most closely fit the observed data. For the fitness function of a given crustal model, we consider the following two measures:

1. The cross-correlation coefficient (CC) between the synthetic and the data (both normalized to unity) for each seismogram. The average CC for all the stations, using both vertical and radial components, is computed and used as the cumulative correlation coefficient (r) for that model. In computing this average, the seismograms are all equally weighted. Also, we preserve the absolute times of the Rayleigh waves by fixing the fitting window for each seismogram.
2. The root-mean-squared (rms) misfit between the data and the synthetics.

We note that both the above-mentioned fitness measures are based on the L2 norm (Parker, 1994). Therefore, these measures selectively fit the larger amplitudes in the seismogram. Thus, the use of an accurate estimate of the source time along with the use of the same time windows in the data and the synthetic, using moveout velocities, allows us to preserve the travel times of the Rayleigh waves in the fitting process. Tests with synthetic data show that the best-fit models, using either of the fitness values, give nearly identical solutions. In a similar analysis, Rodgers and Schwartz (1998) have also reached the same conclusion. As synthetic tests determined that the average correlation coefficient showed faster convergence, we adopted this measure in our fitness measure.

The GA chooses the model with the greatest fitness value (FV) to be the fittest member of the population. Therefore, FV must be calculated to be an ever-increasing function of the fitness measure. A simple solution is to exponentiate the correlation coefficient, r, and set that equal to FV. However, in the presence of several local minima, with fitness values approaching the global minima, premature convergence can occur as the crossover procedure between models with marginally inferior fitness corrupts the algorithm. Increasing the separation between the fitness values of these minima can be accomplished by simply multiplying the exponent by a constant value, which effectively avoids this problem. We therefore chose as the fitness value

$$\mathrm{FV} = \exp(30 \times r).$$

The multiplier, 30, is chosen so that FV is a large number that does not compromise the numerical accuracy of the computer.

Termination of the GA Search. As mentioned earlier, the GA uses random crossover and mutation to explore new regions of the solution space and thereby avoid getting trapped into such a local minima. Because there is no formal way to estimate the global minima using GA, identifying the generation at which to stop the search and accept the solution can be difficult. The final model is usually selected by either terminating the GA after no improvement has been observed for a number of subsequent generations or when the FV is larger than some predetermined value. The latter criteria requires us to make several assumptions regarding the forward problem and the noise levels of the data, which can be *ad hoc*. To avoid such assumptions, we choose the first criteria; that is, we accept the model that best fits the data for at least 20 subsequent generations. This technique can still lead to the choice of a local minima. To avoid such convergence, we can carry out the GA with different starting conditions and then compare the terminated solutions (Levin and Park, 1997). Toward this end, we compute solutions for several different randomizing seed values and use different crossover schemes, that is, crossover occurring at one or two points in the gene. We identify the consistent features of these models and accept the average of the models as the global minima. This approach implicitly assumes that separate GA runs all converge toward the global minima; tests with synthetic data confirm this assumption. Also, the variation of each parameter between different GA runs gives an estimate of the robustness of our selected solution.

Testing the Modeling Algorithm

Synthetic tests have been carried out to investigate the accuracy of the GA modeling. Seismograms are computed for a published model of the Colorado plateau (Wolf and Cipar, 1993) for regional source-to-receiver distances. The resulting synthetic waveforms are then analyzed for the crustal structure using the GA procedure outlined in the previous section. The best-fit model is then compared to the input model to estimate the accuracy of our modeling algorithm. The seismograms are computed for source–receiver distances representative of this study, that is, between 150 and 850 km, and we use an implosion at a depth of 0.5 km as the seismic source. For consistency, the synthetic is processed similar to the data. The tests were carried out using both noise-free synthetics and with seismograms containing additive Gaussian noise. In the following sections, the efficacy and the resolving capability of the modeling algorithm in obtaining the input model from the data is discussed.

Input Model. We use the Chinle-Hanksville, Utah, model of Wolf and Cipar (1993). The model consists of three crustal layers of constant thickness and includes a mid-crustal reflector. This model includes slight velocity gradients in each layer. Velocity gradients within layers are not modeled in our study, and so we use the average layer velocity as a representative value. We also add a sedimentary layer to our input model. Thus the input model (IP) consists of sedimentary, upper, middle, and lower crustal layer thicknesses of 1.5, 10.0, 20.0, and 18.0 km, respectively, with corresponding P-wave velocities are 4.0, 6.0, 6.25, and 6.95 km/sec, respectively (Fig. 4).

One of the important set of input parameters in the modeling algorithm is the selection of limiting values of the model space. We have used conservative estimates in these synthetic tests: ± 0.25 km/sec of the input values for the

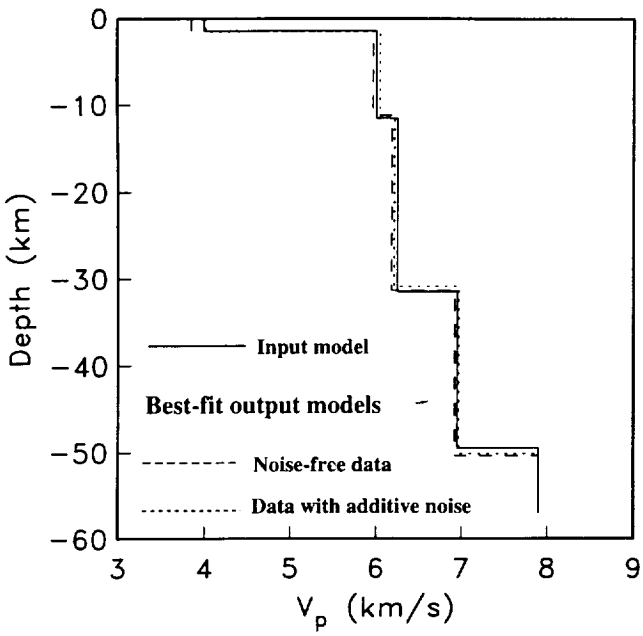

Figure 4. Results from synthetic test of the modeling algorithm developed in this study. We show the best-fit inverted models computed using seismograms constructed from the given input model. Two sets of seismograms, that is, with and without additive noise, are inverted several times each using different randomizing seed values and crossover schemes. We show the average models in this figure. Note that most of the model parameters are retrieved to within ±5% of their input values.

velocities and ±25% of the expected layer thickness are chosen and the GA randomly selects models between these range of values. We add that, typically in the western United States, the crustal properties can be estimated more accurately than these limits. We also use the synthetic experiments to identify the values of crossover and mutation probabilities that can give us a fast convergence to the expected model. Several runs are carried out for both noise-free synthetics and those with additive noise, and the final models are compared. We find that GA runs with mutation probabilities between 0.1 and 0.2 give us the best and nearly identical solutions. We choose a mutation rate of 0.125 for all our modeling experiments. This number is equal to $(1/n)$, where n is the number of model parameters and is expected to give us a more efficient search algorithm (Bäck, 1996). Crossover rates varying between 0.55 and 0.95 are tested. Though higher crossover rates lead to faster convergence (Goldberg, 1989), a rate of 0.95 leads to a premature convergence to a model that is not acceptably close to the solution. These tests suggest that a crossover probability value of 0.85 gives us the most efficient algorithm.

Test with Noise-Free Data. In this experiment, the computed synthetics are modeled to obtain the best-fitting output model (OP). In the absence of noise and given a long enough run time, we expect the solution to ultimately converge to IP because the correlation coefficient for this model should be equal to 1. Due to various factors that include the inherent nonlinearity of the forward problem, the trade-offs between model parameters, and finite computing resources combined with the fact that the convergence rate of GA gets progressively slower as it nears the solution, we choose a solution (OP) that is reasonably close to IP after no improved model has been generated in 20 consecutive generations. The model we chose is generated in the 44th generation and has layer thicknesses of 1.49, 9.7, 20.17, and 19.03 km and velocities of 3.85, 5.96, 6.18, and 6.92 km/sec from the shallowest to the deepest layers, respectively (Fig. 4). A comparison between models OP and IP show that our modeling technique is capable of retrieving the input parameters to within 1 to 4% accuracy. The thickness estimate of the deepest layer is off by up to 5.5%. This is not unexpected given the lack of sensitivity of our dataset to the deeper layers. Figure 5 shows the convergence of the model parameters toward the final solution. We can infer that the GA with noise-free synthetics converges to the solution adequately by the 25th generation.

Test with Noisy Data. For this test, Gaussian random noise is added to the "data" seismograms. A signal-to-noise ratio of 10, approximately equal to the SNR observed in the recorded seismograms, is used. Using this realistic example, we can estimate the effects the trade-offs between model parameters and convergence to a global minimum in the presence of multiple local minima. The GA input parameters are chosen as before with probabilities of crossover and mutation fixed at 0.85 and 0.125, respectively. The GA randomly chooses models where the velocities are allowed to vary to within 0.25 km/sec of input values and the thicknesses can be varied by up to 25%. We carried out 11 different GA runs using different random model generators (by changing the randomizing seed value in the GA) and also by using both one-point and two-point crossover schemes. Figure 6 shows representative models obtained using GA with noisy data. Note that the models all have similar features and are close to the average model. Figure 4 shows the final model for this test, which is the average of the individual models generated from different GA runs. We use the variability of the output model parameters to estimate the errors in these values. The average model has layer thicknesses equal to 1.57 ± 0.07, 9.88 ± 0.39, 19.46 ± 0.38, and 19.23 ± 0.36 km and velocities equal to 4.01 ± 0.04, 6.04 ± 0.02, 6.21 ± 0.01, and 6.97 ± 0.03 km/sec, respectively, from the shallowest to the deepest layers. We accept the standard errors as rough accuracy estimates on our estimated model parameters.

Modeling of Recorded Seismograms

In this section, we present our best-fit estimates of the one-dimensional crustal structures of the Colorado plateau and Great Basin provinces of the western United States. The

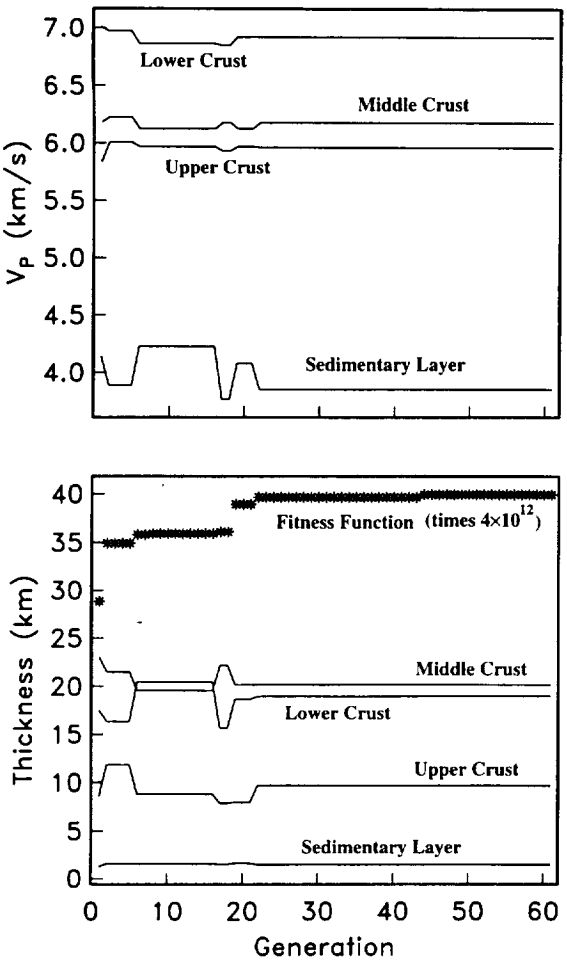

Figure 5. *P*-wave velocity, thickness, and waveform fitness as a function of generation number for a genetic algorithm run with noise-free data (described in text). The crustal model that best fits the synthetic seismograms for an input model (Fig. 7) is plotted for each generation. We note that adequate convergence is reached by the 25th iteration. A one-point crossover scheme is adopted for this run with the crossover probability equal to 0.85 and the mutation probability equal to 0.125 (described in text).

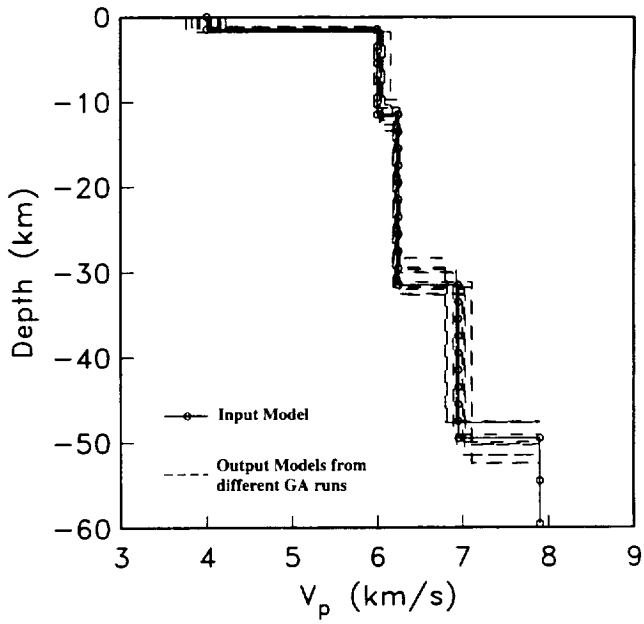

Figure 6. Testing the accuracy of the modeling algorithm in the presence of noise. Noise with signal-to-noise ratio of 10.0 (typical for the Rayleigh waveforms used in this study) is added to the synthetic seismograms computed for the input model (see text). Models generated in 11 GA runs with different randomizing seed values and with both one-point and two-point crossover schemes are shown. The models are similar though the variability between the model values increases for velocities and thicknesses for the deeper layers.

crustal structure in these regions are essentially three-dimensional, and the models presented in this study should be considered a spatial average over the sampled regions. Note that the model parameters along with their error estimates are dependent on the parameterization and the range of their allowable values. As described earlier in the text, values from published literature along with results from sensitivity tests justify our initial values. Though modeling small subsets of data can give us improved fits, we consider all of the stations in a region together to improve spatial averaging.

Crustal Structure of the Colorado Plateau. Seismograms recorded at stations CYF, KNB, LMP, MDW, RCC, SRS, and WMT are used to model the crustal structure of the Colorado plateau. The moveout windows used to excise the Rayleigh waveforms vary from [2.0 5.0] km/sec for RCC at short source–receiver distance to [2.55 3.3] km/sec for the farthest station, KNB. The layer thicknesses are allowed to vary between [1.0 3.0], [8.0 14.0], [15.0 25.0], and [14.0 22.0] km and the *P*-wave velocities between [3.0 5.0], [5.75 6.25], [6.1 6.48], and [6.7 7.0] km/sec, respectively, for the shallowest to the deepest layers.

Our model, which is constructed from a sparse distribution of stations, can be compromised by inadequate spatial sampling. To resolve this issue, we have also carried out a number of experiments by deleting one or more stations and estimate the best-fit model. A number of runs are carried out for each subset of the dataset, and the average model from each of these runs is given in Table 1. We performed three separate sets of GA modeling by (a) removing stations RCC and KNB, located closest and farthest to the source, respectively; (b) removing the data recorded at station RCC that can be biased by high mountains and deep basins located close to the station; and (c) removing stations RCC, WMT, and MDW, where a portion of the source–receiver path does not lie on the Colorado plateau. We conclude from these experiments (Table 1) that the transition zone structure and the complicated seismic anomalies in northwest Utah do not

Table 1
Crustal Models for the Colorado Plateau Region

Layer	Dataset 1: Using All of the Colorado Plateau Stations, Various Seed		Dataset 2: RCC Is Removed from List, Various Seed		Dataset 3: RCC and KNB Are Removed, Various Seed		Dataset 4: Stations KNB, LMP, SRS, and CYF, Various Seed		Colorado Plateau Model: Average of 12 GA Runs	
	h	V_P	h	V_P	h	V_P	h	V_P	h	V_P
Sediments	1.5	3.04	1.5	3.07	1.4	3.1	1.57	3.01	1.5 ± 0.04	3.05 ± 0.02
Upper crust	8.4	5.76	8.3	5.77	8.3	5.9	8.40	5.76	8.3 ± 0.05	5.78 ± 0.01
Middle crust	15.2	6.46	15.3	6.45	15.4	6.4	15.25	6.48	15.3 ± 0.06	6.44 ± 0.01
Lower crust	14.3	6.99	14.6	6.99	14.3	6.95	14.30	6.99	14.4 ± 0.1	6.98 ± 0.002

We show the average models for four separate inversions using subsets of the dataset, using different randomizing seed values, and two different crossover schemes for each dataset. The final Colorado plateau crustal model, which is an average of the separate models generated in each of the runs, is shown in the last column of the table. In this table, h signifies thickness in km, and V_P signifies P-wave velocity in km/sec. The uncertainty in the final model is for this parameterization only and does not cover all possible crustal models.

bias our one-dimensional model. Between the different models, the layer thicknesses are consistent to within 0.2 km, and the individual layer velocities vary by less than 0.12 km/sec. As described earlier, these values are smaller than the ascribed error bars for the model parameters and indicate that each of the solutions are close to the global minima. The average of these models is accepted as the one-dimensional crustal model for the Colorado plateau (Table 1). The largest error is in the estimation of thickness of the lower crust. The primary features of this model are (a) an average crustal thickness of 39.5 km; (b) thin sedimentary layer 1.5 km thick; (c) velocity increases of more than 0.5 km/sec at depths of 10 and 25 km; (d) a fast lower crustal velocity of 7.0 km/sec, and (e) absence of mid-crustal low-velocity layer.

Our crustal thickness value, which is based on the Rayleigh-wave fits, receiver function crustal P and S times, and a fixed upper mantle velocity, is on the lower end of estimates for this region. Recent receiver function results of Sheehan *et al.* (1997) indicate an average crustal thickness of 42 km in the Colorado plateau (assuming an average crustal P-wave velocity of 6.3 km/sec and a Vp:Vs of 1.73). Analysis of refraction data suggest an average Moho depth of about 41.5 km (Roller, 1965). Surface-wave dispersion studies by Keller *et al.* (1976, 1979) and Schneider (1997) indicate a crustal thickness of 40, 45, and 43.5 km, respectively. A reinterpretation of Roller's data by Wolf and Cipar (1993) gives a crustal thickness of 48 km, which is not consistent with our results.

Figure 7 shows a comparison of our crustal models with several published in the literature. Our model most closely resembles the model presented by Keller *et al.* (1976), which was constructed using surface waves in a region of the northern Colorado plateau similar to ours. Our sedimentary layer thicknesses and velocities are in excellent agreement with those presented in studies that have explicitly modeled this layer (Keller *et al.*, 1976, 1979; Roller, 1965). The presence of an upper crustal velocity increase near 10 km depth is

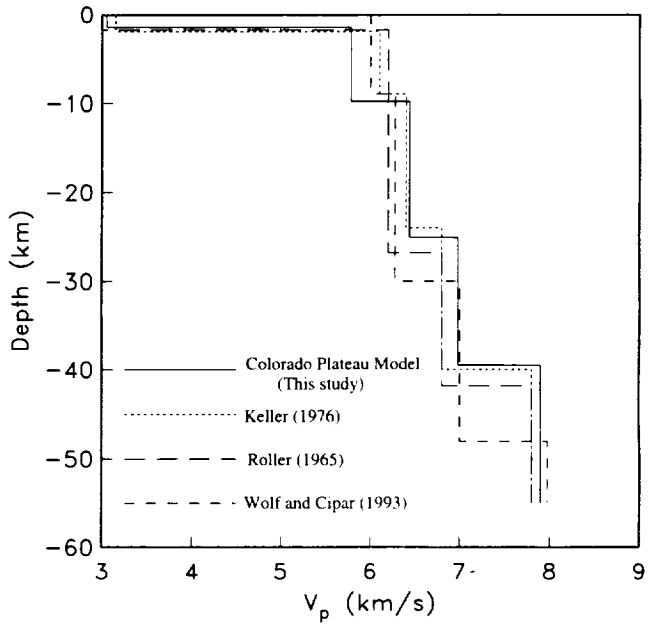

Figure 7. Comparison of our final Colorado plateau model with published models of one-dimensional crustal structure of the same region. The error bounds of our preferred model are given in Table 1.

consistent with the results of Wolf and Cipar (1993) and Keller *et al.* (1976). We also observe a prominent mid-crustal velocity increase at approximately 25 km depth. This layer has been observed by Roller (1965) and Prodehl and Lipman (1989). Published values for this velocity increase range from 27 to 29 km (Allmendinger *et al.*, 1986, from an analysis a COCORP line in Northern Colorado plateau), 30 km (Wolf and Cipar, 1993), 24 km (Keller, 1976), and 29.5 km (Schneider, 1997). We observe a slower upper crustal velocity compared to those reported in the literature. This might be because our paths sample more of the slower velocity sedimentary basins in the northwestern Colorado pla-

teau than the other studies. We observe a very high lower crustal velocity that is consistent with results from other studies of the Colorado plateau crustal structure, for example, 6.8 km/sec (Roller, 1965), 6.8 km/sec (Keller *et al.*, 1976), 6.95 km/sec (Wolf and Cipar, 1993), and 7.0 km/sec (Schneider, 1997). This can explain the unusually small impedance contrast observed for the Moho in a receiver function study of the CPGB stations (Sheehan *et al.*, 1997). Also, the presence of a relatively thin crust under the high standing Colorado plateau lends support to the hypothesis that the high topography of this region is not completely compensated by the crust (Sheehan *et al.*, 1997).

Crustal Structure of the Eastern Great Basin. The crustal structure of the eastern Great Basin province is modeled using data recorded at stations BMN, ELK, GAR, MLC, MNV, RTS, and WCP (Fig. 1). The ray paths sample transects through northern Utah and eastern Nevada. As described earlier, we prescribe a range of values from which the GA randomly chooses the model parameters. For the Great Basin model, the ranges are [1.0 6.0], [4.0 12.0], [8.0 12.0], and [8.0 16.0] km for the thicknesses and [2.5 4.5], [5.8 6.2], [6.1 6.5], and [6.7 7.1] km/sec for the velocities for the shallowest to the deepest layers in the model.

Though using the radial- and vertical-component seismograms for seven stations improves the spatial sampling of the Great Basin region, lack of crossing paths can bias the model search. This is because we are essentially solving for the average crustal structure without complete coverage in a strongly heterogeneous region. For example, the path-to-station WCP crosses the Great Salt Lake Basin, and Rayleigh waves can be strongly affected by this large sedimentary feature. Moreover, significant portions of the paths to the stations ELK, GAR, and WCP traverse the transition zone between the Colorado plateau and Great Basin provinces, which has a somewhat different seismic structure than the Colorado plateau and Great Basin provinces straddling it (Sheehan *et al.*, 1997). Thus, the best-fit models need to be carefully appraised before we accept the average model. Toward this end, we have computed separate GA runs with the stations that have paths mostly in the eastern Great Basin province, that is, BMN, RTS, MLC, and MNV. These models are then compared to those computed for all seven stations. In Table 2, we present the best-fit models. Comparing models computed from the whole dataset and a subset of the data, we note that they are essentially similar though the structure of the sedimentary layer differs. The model computed from the subset of the data consists of a thicker sedimentary layer with faster *P*-wave velocity. This is most probably a reflection of the older basin structures present in northeastern Nevada. We combined the individual models from all the runs and average them for the final Great Basin model (Table 2 and Fig. 8). This model consists of a 35.0-km-thick crust, which is the same as that obtained by Priestley and Brune (1978) and is close to the values presented by Schneider (1997) and Keller (1975), 31.5 km and 29 km, respectively.

Table 2
Crustal Models for the Great Basin Province

Layer	Dataset 1: Using All of the Great Basin Stations, Various Seed		Dataset 2: Using Stations BMN, RTS, MLC, and MNV, Various Seed		Eastern Great Basin Crustal Model: Average of 7 Different GA Runs	
	h	V_P	h	V_P	h	V_P
Sediments	2.8	3.0	3.4	3.7	2.9 ± 0.3	3.1 ± 0.2
Upper crust	8.1	6.1	7.1	6.1	8.0 ± 0.8	6.1 ± 0.02
Middle crust	11.0	6.4	11.7	6.4	11.1 ± 0.3	6.4 ± 0.03
Lower crust	13.0	6.7	13.1	6.8	13.0 ± 0.7	6.8 ± 0.02

We show the final models for two separate runs: (a) the vertical- and radial-component seismograms for all of the Great Basin stations are modeled (dataset 1); (b) when stations for which the seismic paths are mostly in the Great Basin province are modeled (dataset 2). The models are similar and the individual models from each run is averaged to produce our Great Basin crustal model, which is shown in the last column of the table. In this table, h signifies thickness in km and V_P signifies *P*-wave velocity in km/sec. The uncertainty in the final model is for this parameterization only and does not cover all possible crustal models.

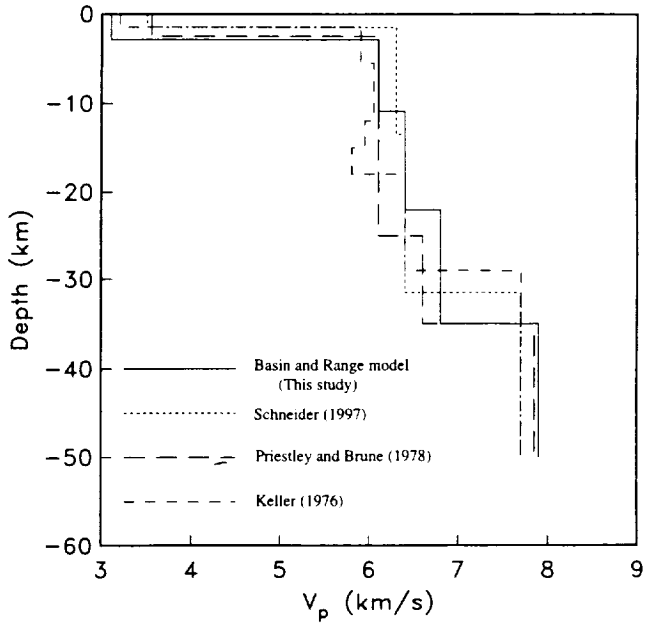

Figure 8. Comparison between our final Great Basin model with several published models of one-dimensional crustal structure of the region. Compared to others, our model shows a slightly thicker sedimentary layer and higher lower crustal velocity. We do not require the crustal low-velocity zone as reported by Keller *et al.* (1976). Uncertainties in our preferred model are given in Table 2.

Our model indicates a 2.9-km-thick sedimentary layer with a *P*-wave velocity of 3.45 km/sec. This is thicker than the shallow layer obtained by Keller *et al.* (1979) but is comparable to the 2.5-km-layer presented by Priestley and Brune (1978) and Song *et al.* (1996). Our upper crust and middle crust layers have an average velocity of approximately 6.1 and 6.4 km/sec, respectively. The average velocity of these two layers of 6.2 km/sec is similar to the values obtained by Priestley and Brune (1978), Song *et al.* (1996), and Schneider (1997). The lower crustal layer has a *P*-wave velocity of 6.8 km/sec. This value is similar to that obtained by Priestley and Brune (1978) but is higher than the 6.4 km/sec obtained by Song *et al.* (1996) and Schneider (1997). We note that the Rayleigh waves arrive later than predicted at stations BMN and ELK, indicating that the crustal velocities are slower or the crust is thicker in the northern Great Basin province, compared to our average model. Finally, we note that the fit to data for the Colorado plateau seismograms is comparatively better than those that traverse the Great Basin province and is probably due to the strong lateral variations of velocity observed in the latter region.

Conclusions

In this study, we have developed a technique to search the parameter space efficiently to model regional broadband seismograms for crustal structure. This technique is based on the GA procedure that generates random models consistent with an allowable set of parameter values. Using an accurate estimate of the source mechanism and location, these models are used to compute synthetic seismograms that are then compared to the recorded data, and the best-fitting model is estimated. This technique assumes that the seismic source model is available, though this is not a necessary condition for this technique. Because having more free variables leads to longer run times, we vary only eight parameters in our search procedure, that is, the thickness and *P*-wave velocities of four crustal layers. Each GA run is carried out with different randomizing seed values and also with different crossover and mutation schemes. This process allows us to avoid converging to a local minima.

Using this technique, we have modeled the Rayleigh waveforms recorded at the CPGB and USNSN stations for separate models of one-dimensional crustal structure in the Colorado plateau and the Great Basin provinces of the western United States. For each of these regions, several independent runs are carried out with subsets of each dataset to estimate the robustness of the final models. The average of the models estimated from each of these runs is accepted as the crustal model for these regions. These one-dimensional models are consistent with other published results of similar structure in these regions. The crust is about 5 km thicker under the Colorado plateau compared to the Great Basin, whereas the latter region has a thicker sedimentary layer. Also, our model indicates a very high lower crustal velocity in the Colorado plateau region.

Acknowledgments

We wish to thank Dave Bahr and T. T. Yu for making important modifications to the development of the genetic algorithm code. We appreciate the help from George Randall in making the reflectivity code available, Chuck Ammon in helping with the use of code, and Craig Jones and Ken Dueker for help in obtaining and analyzing the CPGB data. We thank Bill Walter for giving us the National Seismic Net data. Reviews from Artie Rodgers, Chandan Saikia, and associate editor Bill Walter significantly improved the manuscript. Acknowledgment is made to the donors of The Petroleum Research Fund, administered by the ACS for partial support of this research, the CIRES visiting fellowship award to JB, and also to NASA for Grants NAG5-3054 and NGT5-30025.

References

Allmendinger, R. W., H. Farmer, E. Hauser, J. Sharp, D. Von Tish, J. Oliver, and S. Kaufman (1986). Phanerozoic tectonics of the Basin and Range–Colorado Plateau transition from COCORP data and geologic data: a review, in *Reflection Seismology: The Continental Crust, Geodynamic Series*, vol. 14, M. Barazangi and L. Brown (editors), American Geophysical Union, Washington, D.C., 257–267.

Bäck, Thomas (1996). *Evolutionary Algorithms in Theory and Practice*. Oxford U Press, New York.

Billings, S., B. Kennett, and M. Sambridge (1994). Hypocenter location: genetic algorithms incorporating problem specific information, *Geophys. J. Int.* **118,** 693–706.

Boschetti, F., M. C. Dentith, and R. D. List (1996). Inversion of seismic refraction data using genetic algorithms, *Geophysics* **61,** 1715–1727.

Christensen, N. (1996). Poisson's ratio and crustal seismology, *J. Geophys. Res.* **101,** 3139–3156.

Christensen, N. and W. Mooney (1995). Seismic velocity structure and composition of the continental crust: a global view, *J. Geophys. Res.* **100,** 9761–9788.

Curtis, A., B. Dost, J. Trampert, and R. Snieder (1995). Shear wave velocity structure beneath Eurasia from surface wave group and phase velocities in an inverse problem reconditioned using the genetic algorithm, *EOS* **76,** 386.

Drijkoningen, G. G. and R. S. White (1995). Seismic velocity structure of oceanic crust by inversion using genetic algorithms, *Geophys. J. Int.* **123,** 653–664.

Goldberg, D. E. (1989). *Genetic Algorithms in Search, Optimization, and Machine Learning*, Addison Wesley, Reading, Massachusetts.

Hearn, T., N. Beghoul, and M. Barazangi (1991). Tomography of the western United States from regional arrival times, *J. Geophys. Res.* **96,** 16369–16382.

Jin, S. and R. Madariaga (1993). Background velocity inversion with a genetic algorithm, *Geophys. Res. Lett.* **20,** 93–96.

Jones, C. and the CPGB Field Crew (1996). The 1994-5 Colorado Plateau–Great Basin PASSCAL experiment, *IRIS Newslett.* **XV,** 1–4.

Keller, G. R., R. B. Smith, L. W. Braile, R. Haney, and D. H. Shurbet (1976). Upper crustal structure of the eastern Basin and Range, northern Colorado Plateau, and the middle Rocky mountains from Rayleigh-wave dispersion, *Bull. Seism. Soc. Am.* **66,** 869–876.

Keller, G. R., L. W. Braile, and P. Morgan (1979). Crustal structure, geophysical models and contemporary tectonism of the Colorado Plateau, *Tectonophysics* **61,** 131–147.

Koch, K. and B. Stump (1995). Implications for upper-mantle structure in the western United States from complete far-regional seismograms, *Bull. Seism. Soc. Am.* **85,** 1432–1444.

Levin, V. and J. Park (1997). Crustal anisotropy in the Ural Mountains foredeep from teleseismic Receiver Functions, *Geophys. Res. Lett.* **24,** 1283–1286.

Lomax, A. and R. Snieder (1995). The contrast in upper mantle shear-wave velocity between the East European Platform and tectonic Europe

obtained with genetic algorithm inversion of Rayleigh-wave group dispersion, *Geophys. J. Int.* **123,** 169–182.

Michalewicz, Z. (1996). *Genetic Algorithms + Data Structures = Evolution Programs,* Springer-Verlag, New York.

Nafe, J. E. and C. L. Drake (1957). Variations with depth in shallow and deep water marine sediments of porosity, density, and the velocities of compressional and shear waves, *Geophysics* **22,** 523–552.

Neves, F. A., S. C. Singh, and K. F. Priestley (1996). Velocity structure of upper-mantle transition zones beneath central Eurasia from seismic inversion using genetic algorithms, *Geophys. J. Int.* **125,** 869–878.

Ozalaybey, S., M. K. Savage, A. Sheehan, J. N. Louie, and J. N. Brune (1997). Shear-wave velocity structure in the northern Basin and Range Province from the combined analysis of receiver functions and surface waves, *Bull. Seism. Soc. Am.* **87,** 183–199.

Parker, R. L. (1994). *Geophysical Inverse Theory,* Princeton U Press, Princeton New Jersey.

Patton, H. J. and S. R. Taylor (1984). Q structure of the Basin and Range from surface waves, *J. Geophys. Res.* **89,** 6929–6940.

Pechmann, J. C., W. R: Walter, S. J. Nava, and W. J. Arabasz (1995). The February 3, 1995, M_L 5.1 seismic event in the Trona mining district of southwestern Wyoming, *Seism. Res. Lett.* **66,** 25–34.

Priestley, K. and J. Brune (1978). Surface waves and the structure of the Great Basin of Nevada and western Utah, *J. Geophys. Res.* **83,** 2265–2272.

Prodehl, C. and P. W. Lipman (1989). Crustal structure of the Rocky mountain region, in *Geophysical Framework of the Continental United States,* L. C. Pakiser and W. D. Mooney (Editors), Geological Society of America Memoir, Boulder, Colorado, vol. 172, 249–284.

Randall, G. E. (1994). Efficient calculation of complete differential seismograms for laterally homogeneous earth models, *Geophys. J. Int.* **118,** 245–254.

Rodgers, A. J. and S. Y. Schwartz (1997). Low crustal velocities and mantle lithospheric variations in southern Tibet from regional Pnl waveforms, *Geophys. Res. Lett.* **24,** 9–12.

Rodgers, A. J. and S. Y. Schwartz (1998). Lithospheric structure of the Qiangtang Terrane, northern Tibetan Plateau, from complete Regional waveform modeling: evidence for partial melt, *J. Geophys. Res.* **103,** 7137–7152.

Roller, J. C. (1965). Crustal structure in the eastern Colorado Plateau province from seismic-refraction measurements, *Bull. Seism. Soc. Am.* **55,** 107–119.

Rudnick, R. and D. Fountain (1995). Nature and composition of the continental crust: a lower crustal perspective, *Rev. Geophys.* **33,** 267–309.

Schneider, J. (1997). Crustal and upper mantle structure of the Colorado Plateau and eastern Basin and Range, *Master's Thesis,* University of Colorado at Boulder, 170 pp.

Sen, M. K. and P. L. Stoffa (1992). Rapid sampling of model space using genetic algorithms: examples from seismic waveform inversion, *Geophys. J. Int.* **108,** 281–292.

Sheehan, A. F., C. H. Jones, M. K. Savage, S. Ozalaybey, and J. M. Schneider (1997). Contrasting lithospheric structure beneath the Colorado Plateau and Great Basin: initial results from the Colorado Plateau–Great Basin PASSCAL experiment, *Geophys. Res. Lett.* **24,** 2609–2612.

Song, X. J., D. V. Helmberger, and L. Zhao (1996). Broad-band modeling of regional seismograms: the Basin and Range crustal structure, *Geophys. J. Int.* **125,** 15–29.

Stoffa, P. L. and M. K. Sen (1991). Nonlinear multiparameter optimization using genetic algorithms: inversion of plane-wave seismograms, *Geophysics* **56,** 1794–1810.

Stoffa, P. L., M. K. Sen, C. Valera, and R. K. Chunduru (1994). Geophysical applications of global optimization methods, *European Assoc. Explor. Geophys.* **56,** 134.

Winchester, J. P., K. C. Creager, and T. J. McSweeney (1993). Better alignment through better breeding: phase alignment using genetic algorithms and cross-correlation techniques, *EOS* **74,** 394.

Wolf, L. W. and J. J. Cipar (1993). Through thick and thin: a new model for the Colorado Plateau from seismic refraction data from Pacific to Arizona Crustal Experiment, *J. Geophys. Res.* **98,** 19881–19894.

Wright, A. H. (1991). Genetic algorithms for real parameter optimization, in *Foundations of Genetic Algorithms,* Gregory J. E. Rawlins (Editors), Morgan Kaufmann Publishers, San Mateo, California.

Yu, T. T. (1995). Crustal deformation due to a dipping fault in an elastic gravitational layer overlying a viscoelastic gravitational halfspace: models and applications, *Ph.D. Thesis,* University of Colorado at Boulder.

Zandt, G., S. C. Myers, and T. C. Wallace (1995). Crust and mantle structure across the Basin and Range–Colorado Plateau boundary at 37° N latitude and implications for Cenozoic extensional mechanism, *J. Geophys. Res.* **100,** 10529–10548.

Zhou, R., F. Tajima, and P. L. Stoffa (1995). Application of genetic algorithms to constrain near-source velocity structure for the 1989 Sichuan earthquakes, *Bull. Seism. Soc. Am.* **85,** 590–605.

CIRES
University of Colorado
Boulder, Colorado

Manuscript received 12 November 1997.